The Importance of Equilibrium Fluctuations between Most Stable Conformers on the Control of the Reaction Mechanism

Bruno S. Souza and Faruk Nome

Electronic Supporting Information

1. **Full scale mass spectra of the hydrolysis products of 1AC2NA and 1AC2NA in natural and ^{18}O labeled water**

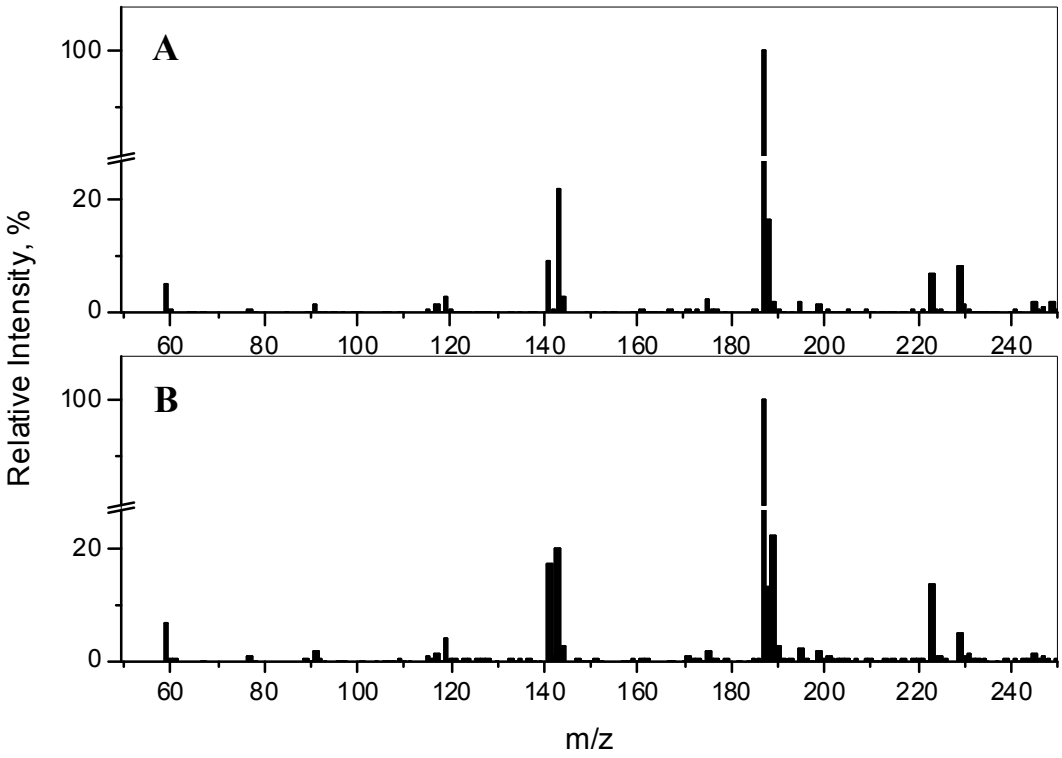

Figure S1. ESI-MS data for hydrolysis products of **1AC2NA** in (A) H_2O; (B) 20% ^{18}O labeled water.

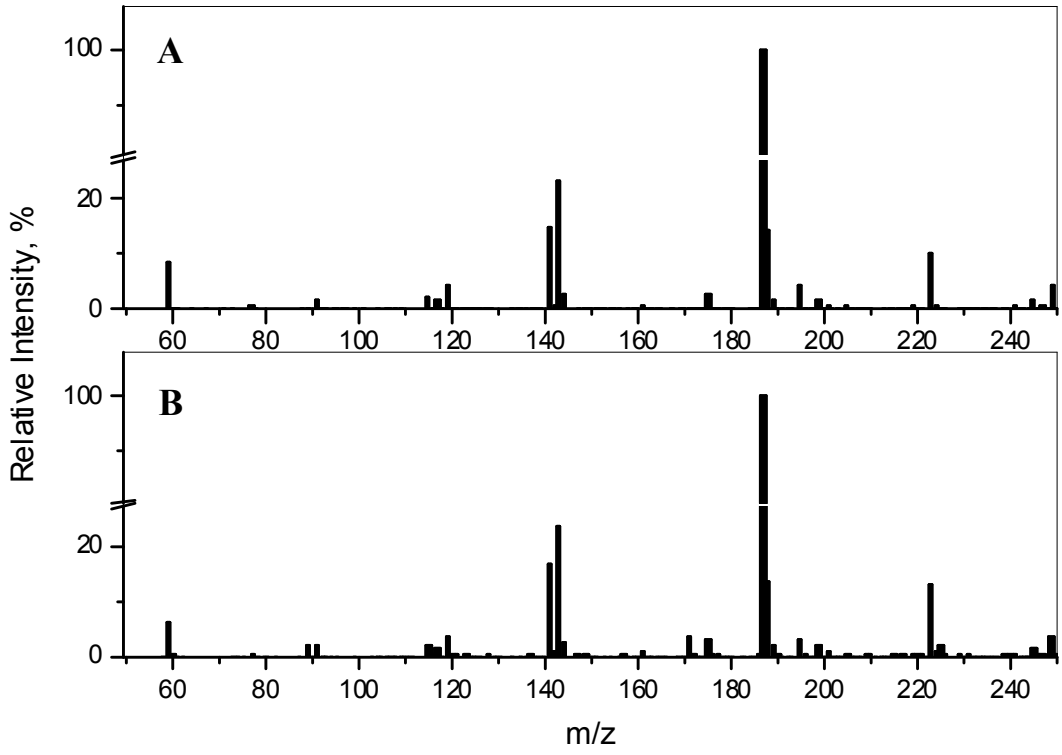

Figure S2. ESI-MS data for hydrolysis products of **3AC2NA** in (A) H_2O; (B) 20% ^{18}O labeled water.

2. Kinetic results

Table S1 - Rate constants as a function of pH for the hydrolysis of 1AC2NA and 3AC2NA in water at 45 °C and ionic strength 1.0 M (KCl).

1AC2NA		3AC2NA	
pH	**$10^5\ k_{obs}/s^{-1}$**	**pH**	**$10^5\ k_{obs}/s^{-1}$**
0.00	3.00	0.00	15.7
0.52	1.21	1.00	2.04
1.00	0.872	1.50	0.656
1.10	0.748	1.69	0.505
1.50	0.796	2.20	0.336
2.20	1.99	2.40	0.309
2.41	2.61	2.79	0.472
2.60	3.34	3.06	0.519
2.81	4.29	3.49	0.735
3.01	5.08	3.72	0.914
3.49	6.98	4.21	1.18
4.03	8.05	4.36	1.22
4.50	8.32	4.99	1.38
5.01	8.50	6.01	1.45
5.47	7.93	7.02	1.50
6.01	8.22	8.51	2.31
6.51	8.25	8.90	3.17
7.49	8.37	11.5	354
8.12	8.88	11.5	267
8.61	9.50	12.5	3130
8.90	8.59		
10.00	9.14		
11.50	91.8		
12.00	183		
12.50	525		

Table S2. Rate constants as a function of temperature for the hydrolysis of 1AC2NA and 3AC2NA in water at pH 6.65 (phosphate buffer 0.01M) and ionic strength 1.0 M (KCl).

1AC2NA		3AC2NA	
T (K)	**$10^5\ k_{obs}/s^{-1}$**	**T (K)**	**$10^5\ k_{obs}/s^{-1}$**
318.15	8.33	318.15	1.46
323.15	17.40	323.15	2.44
333.15	54.80	333.15	5.74
343.15	215.00	343.15	14.9

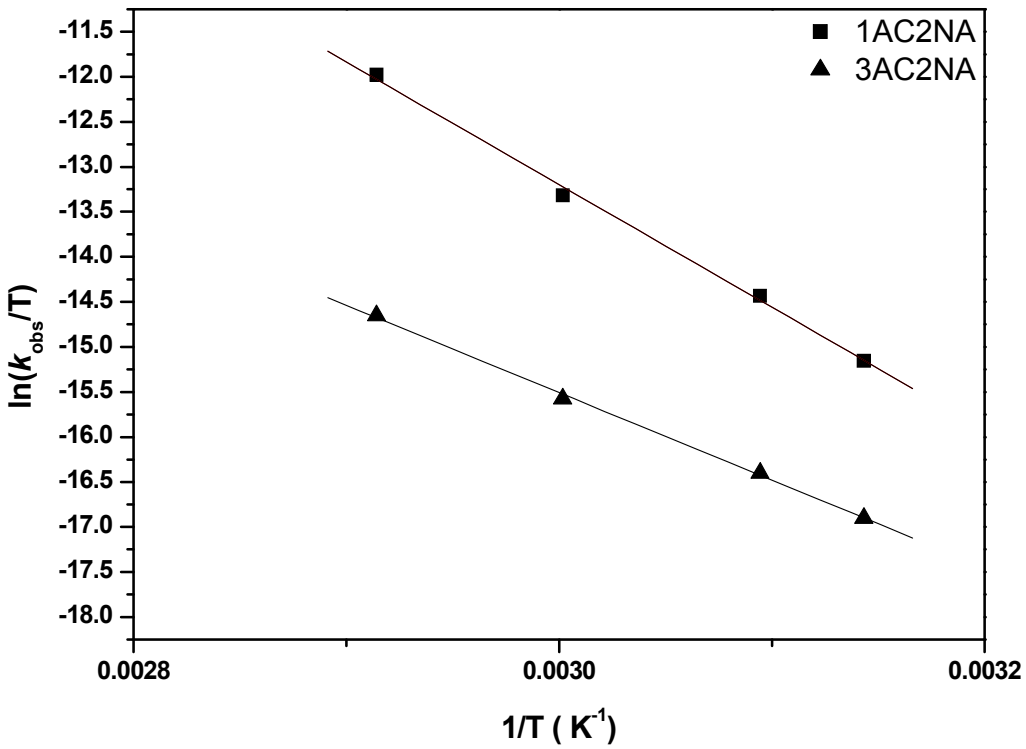

-Figure S3. Eyring plot for the hydrolysis of 1AC2NA and 3AC2NA at pH 6.65 (phosphate buffer 0.01M) and ionic strength 1.0 M (KCl).

3. Spectrofluorimetric titration of 1OH2NA and 3OH2NA

The spectrofluorimetric titration results were fitted by using the following equation based on the following equilibrium:

$$I = A\left(\frac{[H^+]}{K_{a1}+[H^+]}\right) + B\left(\frac{K_{a1}}{K_{a1}+[H^+]}\right)\left(\frac{[H^+]}{K_{a2}+[H^+]}\right) + C\left(\frac{K_{a2}}{K_{a2}+[H^+]}\right)$$

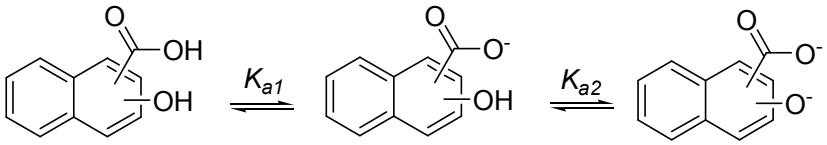

where:

I- Fluorescence intensity;

A- Fluorescence intensity of the neutral specie;

B- Fluorescence intensity of the monoanionic specie;

C- Fluorescence intensity of the dianionic specie;

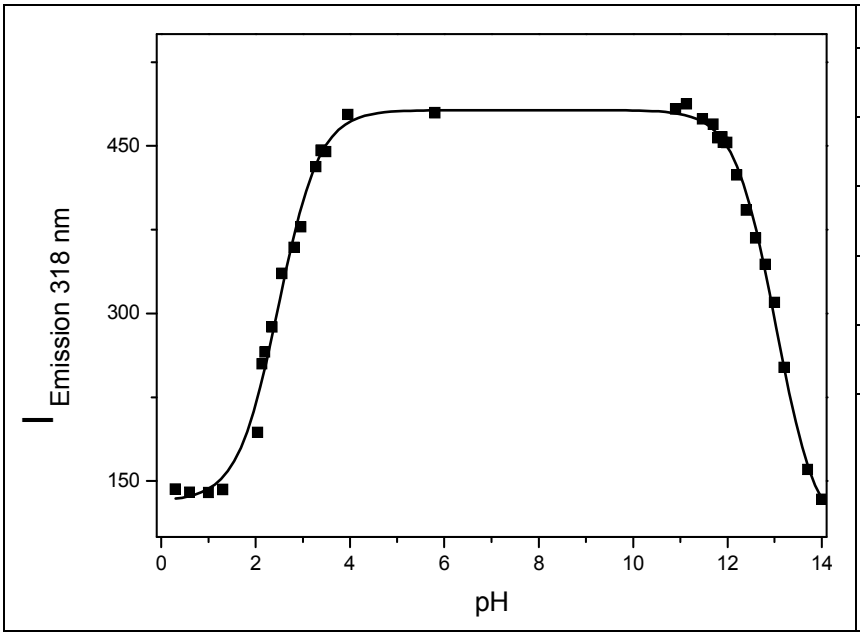

Fitting	results
pK_{a1}	2.48±0.03
pK_{a2}	13.02±0.04
A	132.04±5.70
B	482.00±3.55
C	97.17±12.17
R	0.992

- Figure S4. Plot of fluorescence emission intensity versus pH for the titration of 66.66 μM solution of 1OH2NA, μ=1.0 M (KCl), room temperature.

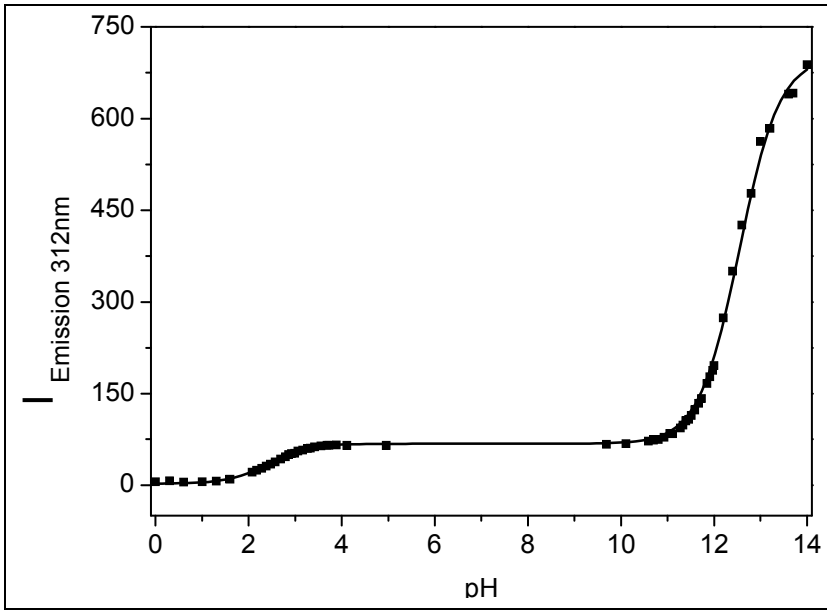

Fitting	results
pK_{a1}	2.53±0.07
pK_{a2}	12.52±0.03
A	3.15±0.08
B	70.00±0.60
C	694.30±3.74
R	0.997

- Figure S5. Plot of fluorescence emission intensity versus pH for the titration of 66.66 μM solution of 3OH2NA, μ=1.0 M (KCl), room temperature.

4 Statistical Analysis of the O7-C4 distance

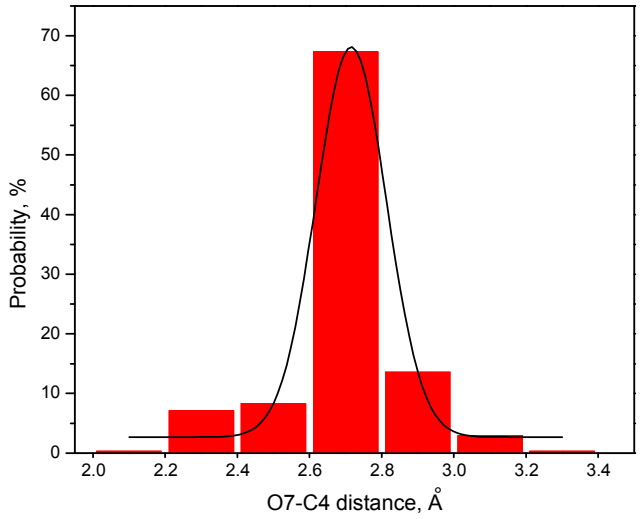

Model	Gauss		
Equation	y=y0 + (A/(w*sqrt(PI/2)))*exp(-2*((x-xc)/w)^2)		
Reduced Chi-Sqr	10.10482		
Adj. R-Square	0.98225		
		Value	Standard Error
K	y0	2.67962	1.59551
K	xc	2.61565	0.01393
K	w	0.19487	0.01726
K	A	15.98835	1.60398
K	sigma	0.09743	
K	FWHM	0.22944	
K	Height	65.46435	

Figure S6. Statistical analysis of the ~ 800 strucutres obtained from the RPES of 1AC2NA. Probability derived from Boltzmann distribution function.

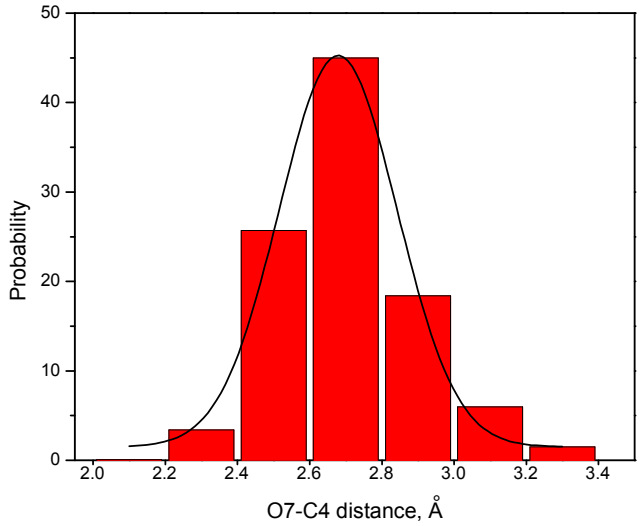

Model	Gauss		
Equation	y=y0 + (A/(w*sqrt(PI/2)))*exp(-2*((x-xc)/w)^2)		
Reduced Chi-Sqr	4.07122		
Adj. R-Square	0.98514		
		Value	Standard Error
K	y0	1.50584	1.21322
K	xc	2.57891	0.00898
K	w	0.32622	0.02028
K	A	17.89407	1.32119
K	sigma	0.16311	
K	FWHM	0.38409	
K	Height	43.76656	

Figure S7. Statistical analysis of the ~ 800 strucutres obtained from the RPES of 3AC2NA. Probability derived from Boltzmann distribution function.

5 Characterization of 1-acetoxy-2-naphthoic acid (1AC2NA)

^{1}H NMR (400 MHz, Acetone *d*6, TMS): 8,16 (1H, d, *J* = 8,26); 8,07 (1H, d, *J* = 8,67); 8,03 (1H, d, *J* = 7,97); 7,91 (1H, d, *J* = 8,67); 7,70 (1H, t, *J* = 7,43); 7,65 (1H, t, *J* = 7,65), 2,46 (3H, s). ν_{max} (KBr) 3080-2600 , 1766, 1683, 1296 and 1207 cm-1. m/z (ESI-MS, negative mode, mobile phase H_2O/CH_3CN 1:9): 270 (4,60%, M - H + CH3CN), 229 (32,5%, M - H), 187 (100%, M – CH_3CO).

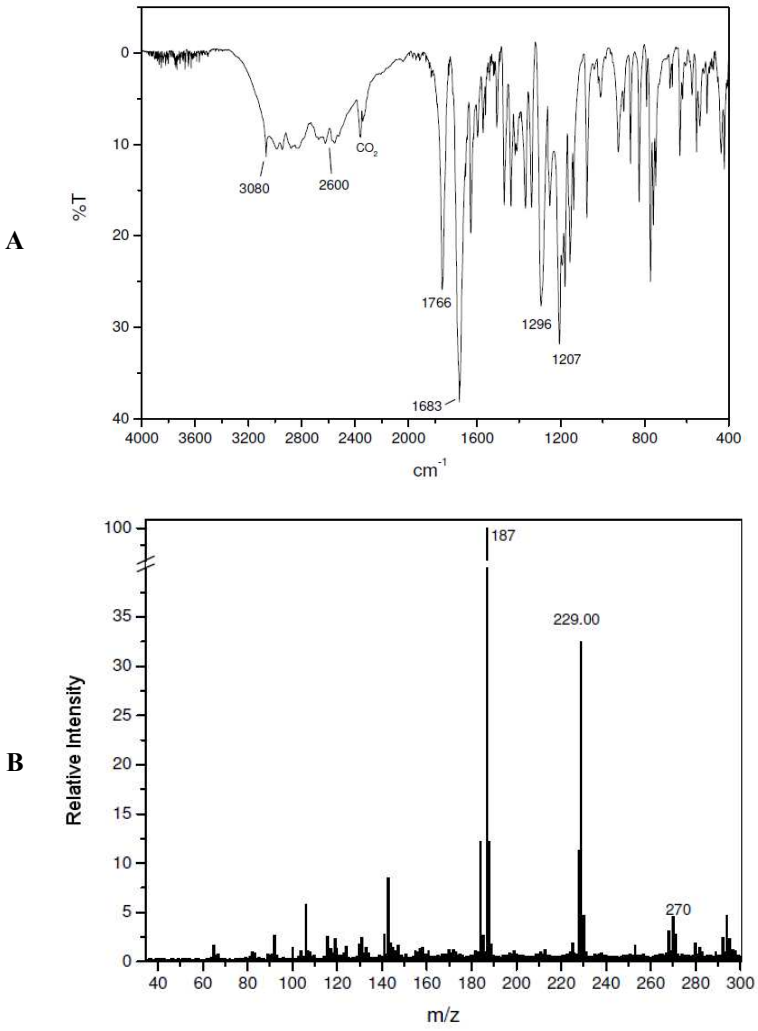

- Figure S8. (A) FTIR and (B) ESI-MS spectra of 1AC2NA.

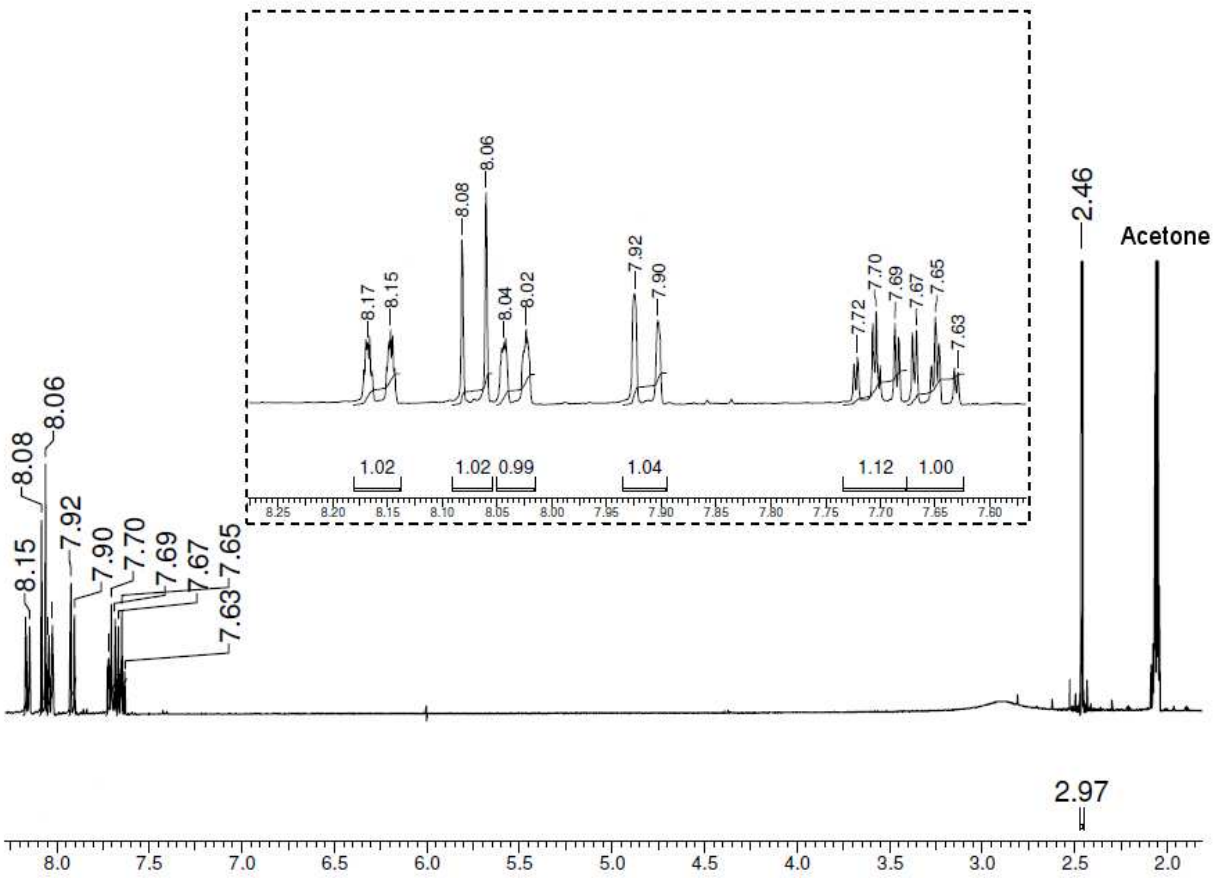

- Figure S9. ^{1}H NMR (400 MHz, Acetone d_6) of 1AC2NA.

6 Characterization of 3-acetoxy-2-naphthoic acid (3AC2NA)

^{1}H NMR (400 MHz, Acetone *d*6, TMS): 8,69 (1H, s); 8,11 (1H, d, *J* = 8,12); 7,97 (1H, d, *J* = 8,17); 7,68 (2H, m); 7,61 (1H, t, *J* = 7,37), 2,30 (3H, s). ν_{max} (KBr) 3084-2800, 1764, 1700, 1294, 1207 cm^{-1}. m/z (ESI-MS, negative mode, mobile phase H_2O/CH_3CN 1:9): 270 (17,80%, M - H + CH3CN), 229 (25%, M - H), 187 (100%, M – CH_3CO).

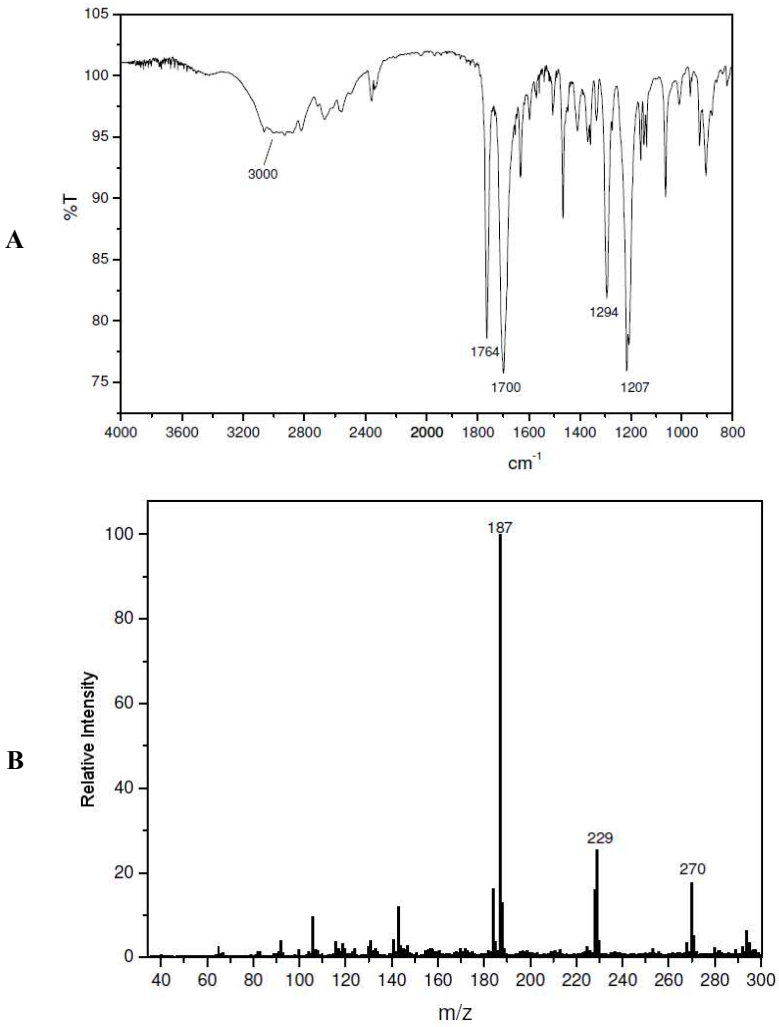

- Figure S10. (A) FTIR and (B) ESI-MS spectra of 3AC2NA.

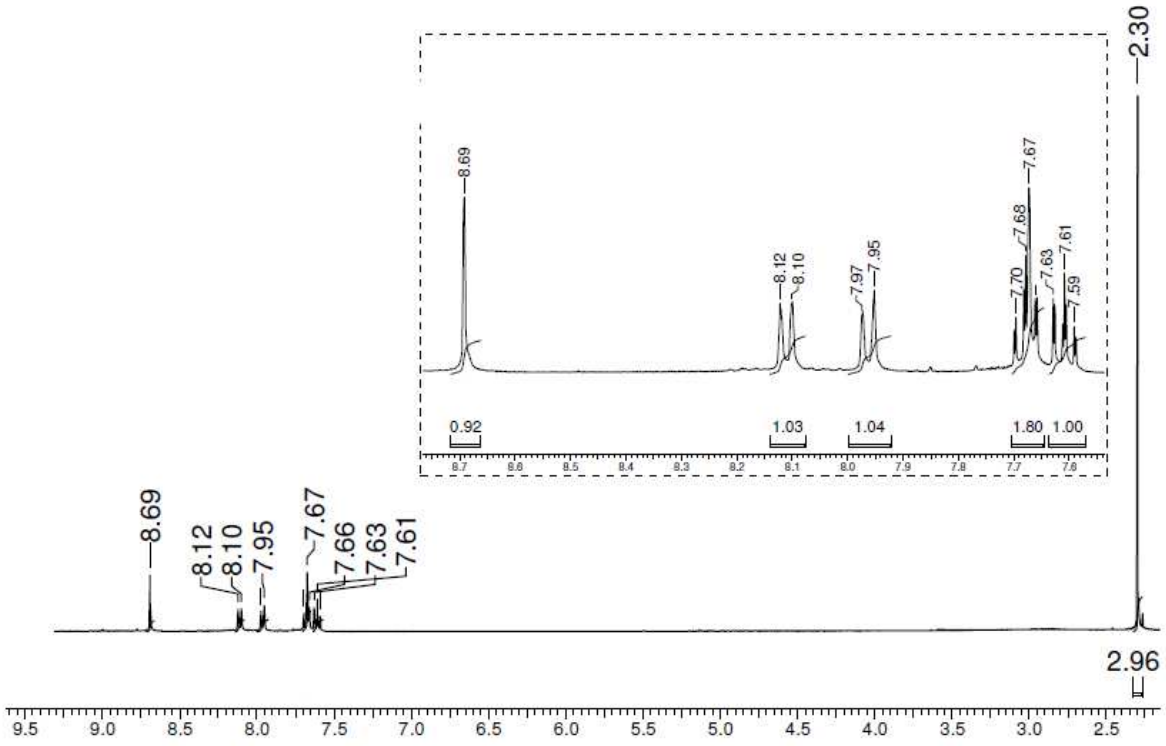

- Figure S11. ^{1}H NMR (400 MHz, Acetone d_6) of 3AC2NA.

7 Relaxed potential energy surface (RPES)

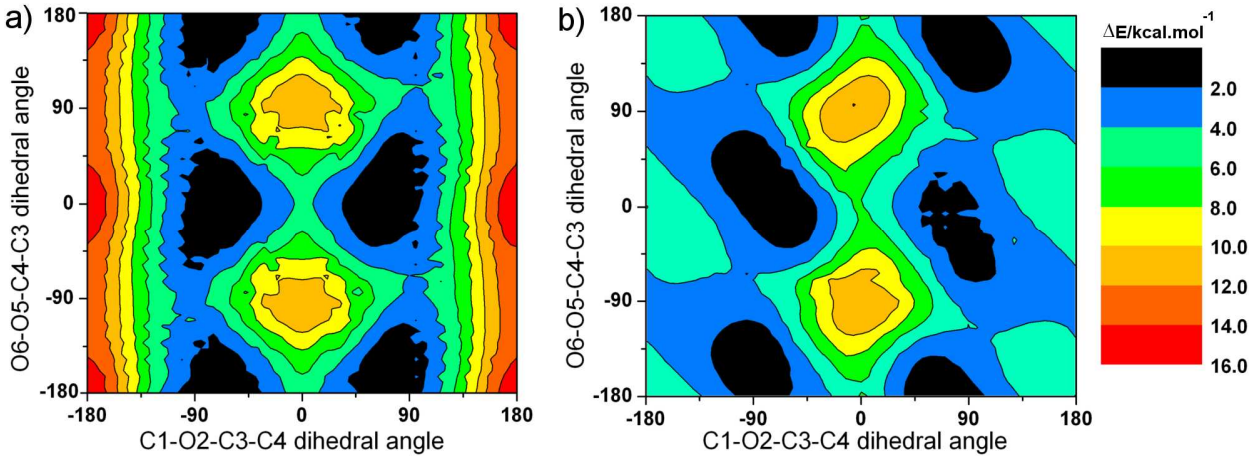

Figure S12. 1AC2NA **(a)** and 3AC2NA (**b)** RPES 2D plot.

8 B3LYP/PCM/6-311++G(2df,p) Cartesian coordinates of 1AC2NA and 3AC2NA

1AC2NA				3AC2NA			
C	-2.315512000	-1.645813000	-0.511066000	C	-4.340966000	0.167559000	0.279154000
C	-0.958788000	-1.454426000	-0.595980000	C	-3.285690000	1.042970000	0.333330000
C	-0.391888000	-0.182197000	-0.332842000	C	-1.961669000	0.597601000	0.087609000
C	-1.256873000	0.902582000	0.006520000	C	-1.743556000	-0.779867000	-0.218102000
C	-2.651444000	0.666701000	0.088842000	C	-2.854244000	-1.658996000	-0.269098000
C	-3.171188000	-0.578136000	-0.161881000	C	-4.122945000	-1.196012000	-0.024792000
C	1.001941000	0.075146000	-0.395550000	C	-0.851935000	1.475322000	0.122121000
C	1.539388000	1.322786000	-0.193251000	C	0.434037000	1.037262000	-0.095592000
C	0.653553000	2.384800000	0.121585000	C	0.619200000	-0.335656000	-0.385664000
C	-0.694611000	2.182640000	0.237456000	C	-0.420751000	-1.217701000	-0.465812000
C	3.032226000	1.615362000	-0.322919000	H	-5.349411000	0.518873000	0.469341000
O	3.328724000	2.637456000	-0.993720000	H	-3.450237000	2.090719000	0.565208000
O	3.829321000	0.836735000	0.250298000	H	-2.684505000	-2.705350000	-0.503194000
O	1.843756000	-0.971856000	-0.790453000	H	-4.966317000	-1.877002000	-0.064341000
C	2.377721000	-1.778490000	0.160504000	H	-0.232288000	-2.255087000	-0.723051000
C	3.413601000	-2.685344000	-0.431821000	C	1.607021000	2.008694000	-0.004854000
O	2.037672000	-1.758072000	1.316972000	O	2.563952000	1.665020000	0.729660000
H	-2.735646000	-2.624841000	-0.714653000	O	1.504313000	3.078349000	-0.657264000
H	-0.316697000	-2.280463000	-0.871080000	H	-1.024453000	2.526800000	0.327883000
H	-3.303434000	1.493949000	0.351343000	O	1.908138000	-0.773989000	-0.717612000
H	-4.240776000	-0.745993000	-0.097296000	C	2.661261000	-1.391528000	0.224369000
H	1.073067000	3.372812000	0.269661000	C	4.046330000	-1.648754000	-0.288899000
H	-1.353700000	3.005966000	0.493676000	O	2.250015000	-1.689850000	1.318207000
H	3.655644000	-3.479642000	0.267474000	H	4.564496000	-2.337065000	0.371653000
H	3.069830000	-3.102618000	-1.376876000	H	4.015290000	-2.045354000	-1.302409000
H	4.308228000	-2.095028000	-0.634633000	H	4.586398000	-0.701219000	-0.319893000

9 B3LYP/6-311++G(2df,p) Cartesian coordinates of 1AC2NA and 3AC2NA

1AC2NA				3AC2NA			
C	3.202202000	-1.619403000	-0.334771000	C	-3.292493000	1.761703000	-0.211847000
C	4.020816000	-0.512818000	-0.024338000	C	-3.270220000	0.349281000	-0.186010000
C	3.454143000	0.716731000	0.200881000	C	-2.073758000	-0.321769000	-0.140024000
C	2.052880000	0.903256000	0.127683000	C	-0.843897000	0.380922000	-0.119478000
C	1.226046000	-0.218579000	-0.184312000	C	-0.863279000	1.809022000	-0.148221000
C	1.839365000	-1.474280000	-0.413185000	C	-2.116648000	2.469294000	-0.193129000
C	1.436137000	2.158579000	0.344913000	C	0.409034000	-0.268270000	-0.070593000
C	0.078675000	2.293481000	0.240033000	C	1.570642000	0.456592000	-0.064488000
C	-0.772781000	1.200654000	-0.056525000	C	1.585122000	1.876251000	-0.083658000
C	-0.179444000	-0.025514000	-0.250876000	C	0.364356000	2.508685000	-0.116229000
C	-2.296104000	1.475765000	-0.180629000	C	2.879827000	2.738280000	-0.066730000
O	-3.057560000	0.510016000	0.047951000	O	2.766753000	-0.239603000	0.073823000
O	-2.579840000	2.650061000	-0.490618000	O	3.910518000	2.181894000	-0.509149000
O	-0.950428000	-1.122617000	-0.626798000	O	2.732209000	3.895686000	0.368502000
C	-1.668201000	-1.772374000	0.340898000	C	3.545114000	-0.419239000	-1.037517000
C	-2.812706000	-2.521894000	-0.275300000	O	3.110648000	-0.433928000	-2.156582000
O	-1.361182000	-1.782331000	1.501267000	C	4.968350000	-0.679698000	-0.640893000
H	3.653079000	-2.588429000	-0.508313000	H	-4.240959000	2.282832000	-0.247117000
H	5.094812000	-0.637102000	0.036319000	H	-4.201776000	-0.202555000	-0.203045000
H	4.077259000	1.570800000	0.439336000	H	-2.055275000	-1.405109000	-0.120583000
H	1.211978000	-2.321590000	-0.648230000	H	-2.128304000	3.552298000	-0.212787000
H	2.058711000	3.013963000	0.581191000	H	0.460778000	-1.348951000	-0.038939000
H	-0.405026000	3.252929000	0.359241000	H	0.372264000	3.590876000	-0.095604000
H	-3.187868000	-3.264426000	0.423797000	H	5.506557000	-1.132253000	-1.469406000
H	-2.512819000	-2.991638000	-1.211543000	H	5.017007000	-1.314797000	0.242934000
H	-3.582042000	-1.780478000	-0.490419000	H	5.398678000	0.290862000	-0.394404000

10 Gaussian full reference

Gaussian 03, Revision D.01, M. J. Frisch, G. W. Trucks, H. B. Schlegel, G. E. Scuseria, M. A. Robb, J. R. Cheeseman, J. A. Montgomery, Jr., T. Vreven, K. N. Kudin, J. C. Burant, J. M. Millam, S. S. Iyengar, J. Tomasi, V. Barone, B. Mennucci, M. Cossi, G. Scalmani, N. Rega, G. A. Petersson, H. Nakatsuji, M. Hada, M. Ehara, K. Toyota, R. Fukuda, J. Hasegawa, M. Ishida, T. Nakajima, Y. Honda, O. Kitao, H. Nakai, M. Klene, X. Li, J. E. Knox, H. P. Hratchian, J. B. Cross, V. Bakken, C. Adamo, J. Jaramillo, R. Gomperts, R. E. Stratmann, O. Yazyev, A. J. Austin, R. Cammi, C. Pomelli, J. W. Ochterski, P. Y. Ayala, K. Morokuma, G. A. Voth, P. Salvador, J. J. Dannenberg, V. G. Zakrzewski, S. Dapprich, A. D. Daniels, M. C. Strain, O. Farkas, D. K. Malick, A. D. Rabuck, K. Raghavachari, J. B. Foresman, J. V. Ortiz, Q. Cui, A. G. Baboul, S. Clifford, J. Cioslowski, B. B. Stefanov, G. Liu, A. Liashenko, P. Piskorz, I. Komaromi, R. L. Martin, D. J. Fox, T. Keith, M. A. Al-Laham, C. Y. Peng, A. Nanayakkara, M. Challacombe, P. M. W. Gill, B. Johnson, W. Chen, M. W. Wong, C. Gonzalez, and J. A. Pople, Gaussian, Inc., Wallingford CT, 2004.